UDC

COPPER(II) AND COBALT(II) COMPLEXES OF 2,6-DIACETYLPYRIDINE BIS(*O*-METHYLOXIME): A THEORETICAL INVESTIGATION

© 2012 **N. Özdemir[1]*, O. Dayan[2], M. Dinçer[1], B. Çetinkaya[3]**

[1]*Department of Physics, Faculty of Arts and Sciences, Ondokuz Mayıs University, Kurupelit, Samsun, Turkey*
[2]*Department of Chemistry, Faculty of Arts and Sciences, Çanakkale Onsekiz Mart University, Çanakkale, Turkey*
[3]*Department of Chemistry, Science Faculty, Ege University, İzmir, Turkey*

The molecular geometries and vibrational frequencies of the title compounds in the ground state are calculated using the Hartree-Fock (HF) and density functional theory (DFT/B3LYP) methods with the LANL2DZ basis set and compared with the experimental data. The calculated results show that the optimized geometries can well reproduce the crystal structural parameters, and the theoretical vibrational frequencies show good agreement with the experimental values. The energetic behavior of the title compounds in solvent media is examined using the B3LYP method with the LANL2DZ basis set by applying the Onsager and polarizable continuum model (PCM). In addition, molecular electrostatic potential (MEP) and frontier molecular orbital (FMO) analyses of the title compounds are investigated by theoretical calculations.

K e y w o r d s: 2,6-diacetylpyridine bis(*O*-methyloxime), IR spectroscopy, *ab initio* calculations, molecular electrostatic potential, frontier molecular orbitals.

INTRODUCTION

Remarkable advances in homogenous catalyst technology have recently been achieved with systems comprising late transition metals and 2,6-diiminopyridyl ligands [1—3]. Various 2,6-diacetylpyridine diimines have been studied as catalysts for the polymerization and epoxidation of alkenes [4—6]. Upon coordination to a transition metal, the bis(chelate) framework may confer interesting stoichiometric and catalytic properties on such complexes [7, 8]. This family of catalysts has attracted great interest in both academia and industry [9, 10].

In the previous publications, the crystal structures of the title compounds, namely dichloro[(1*E*,1′*E*)-1,1′-(pyridine-2,6-diyl)diethanone bis(*O*-methyloxime)-$\kappa^3 N^1, N^2, N^6$]copper(II) (**1**) [11] and dichloro[(1*E*,1′*E*)-1,1′-(pyridine-2,6-diyl)diethanone bis(*O*-methyloxime)-$\kappa^3 N^1, N^2, N^6$] cobalt(II) (**2**), have been studied [12]. To the best of our knowledge, no estimates of theoretical results for the compounds have been reported so far. In this study, the geometrical parameters, fundamental frequencies, and some molecular properties of the compounds in the ground state were calculated using the Hartree–Fock (HF) and density functional theory (DFT/B3LYP) methods with the LANL2DZ basis set and the results are compared with the experimental findings.

The DFT method combines accuracy with computational speed and ease of use. This is particularly true for hybrid DFT methods, which have consistently been shown to be highly reliable. Of all hybrid DFT methods, the B3LYP functional is the most widely used [13] and yields accurate results for many systems containing transition metal atoms [14]. The choice of the LANL2DZ basis set for metal complexes was preferred, based on the accurate results obtained in the description of metal-ligand interactions [15, 16].

---

* E-mail: namiko@omu.edu.tr

COMPUTATIONAL DETAILS

The molecular structures of the compounds in the ground state were optimized using the unrestricted Hartree—Fock (UHF) and hybrid density functional theory (DFT/UB3LYP) methods [17, 18] with the widely used LANL2DZ basis set [19]. Vibrational frequencies for the optimized molecular structures of the title compounds were calculated using these methods and then scaled by 0.88 [20] and 0.975 [21] respectively. All the calculations were performed using the GaussView molecular visualization program [22] and the Gaussian 03 program package [23] without specifying any symmetry for the molecules. In order to investigate the solvent effect on the total energy and dipole moment, we have also carried out optimization calculations in three kinds of solvent [$\varepsilon = 4.90$, chloroform ($CHCl_3$); $\varepsilon = 32.63$, methanol (CH_4O), $\varepsilon = 78.39$, water (H_2O)] at the B3LYP/LANL2DZ level using Onsager [24] and Polarizable Continuum Model (PCM) [25] methods. All geometry optimization calculations were followed by vibrational frequency calculations to ensure that no imaginary vibrational frequency was present in optimized geometries.

RESULTS AND DISCUSSION

Theoretical structures. Full crystallographic data were deposited with the Cambridge Crystallographic Database; CCDC deposition numbers are 616123 and 621254 for compounds **1** and **2** respectively. The final atomic coordinates for both compounds are given in Table 1, while the experimental and optimized structures are shown in Figs. 1 and 2. For compound **1**, bond distances agree within ca. 0.17 Å for HF and 0.09 Å for B3LYP, while the largest deviation of bond angles appears to be about 12.54° for HF and 13.80° for B3LYP. Using the root mean square error (RMSE) for evaluation, the B3LYP method best predicts the bond distances, with a value of ca. 0.052 Å. However, the HF method
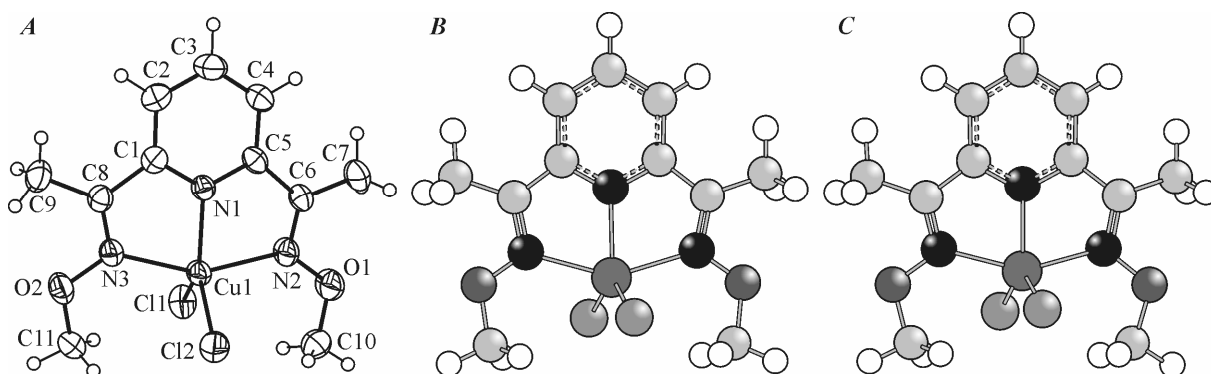

Fig. 1. Experimental geometric structure of complex **1** (*A*); theoretical geometric structure of complex **1** at the UHF/LANL2DZ level (*B*); theoretical geometric structure of compound **1** at the UB3LYP/LANL2DZ level (*C*)

Fig. 2. Experimental geometric structure of complex **2** (*A*); theoretical geometric structure of complex **2** at the UHF/LANL2DZ level (*B*); theoretical geometric structure of compound **2** at the UB3LYP/LANL2DZ level (*C*)
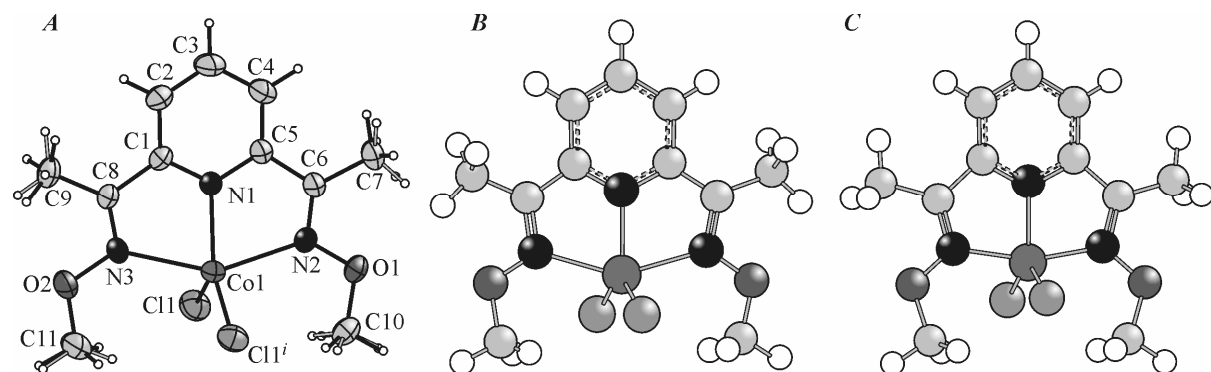
Table 1

Final Atomic Coordinates of Compounds **1** *and* **2**

Atom	Compound **1**			Compound **2**		
	x	*y*	*z*	*x*	*y*	*z*
Cu/Co	0.77272(2)	0.74169(2)	0.007730(19)	0.391530(17)	0.2500	0.78054(3)
Cl1	0.70923(6)	0.94929(5)	–0.03353(5)	0.32820(3)	–0.00051(7)	0.76344(5)
Cl2/Cl1[i]	0.85236(5)	0.67678(5)	0.18535(4)	0.32820(3)	0.5005	0.76344(5)
O1	0.47555(17)	0.7102(2)	–0.01732(17)	0.41761(11)	0.2500	0.46697(18)
O2	1.06819(14)	0.82100(15)	0.06380(14)	0.35399(10)	0.2500	1.08285(18)
N1	0.75633(15)	0.61571(14)	–0.10487(12)	0.50325(10)	0.2500	0.81036(18)
N2	0.57576(16)	0.67441(16)	–0.04581(14)	0.40510(10)	0.2500	0.98617(19)
N3	0.95809(17)	0.74838(14)	0.00503(14)	0.44555(11)	0.2500	0.5878(2)
C1	0.86158(18)	0.59136(17)	–0.12398(14)	0.55050(13)	0.2500	0.7138(2)
C2	0.8548(2)	0.50059(19)	–0.20008(17)	0.62604(16)	0.2500	0.7333(3)
H2	0.9286	0.4816	–0.2126	0.6587	0.2500	0.6661
C3	0.7353(2)	0.4393(2)	–0.25663(18)	0.65238(16)	0.2500	0.8530(3)
H3	0.7285	0.3783	–0.3082	0.7033	0.2500	0.8671
C4	0.6255(2)	0.4671(2)	–0.23789(16)	0.60425(14)	0.2500	0.9528(3)
H4	0.5445	0.4270	–0.2771	0.6218	0.2500	1.0343
C5	0.63961(18)	0.55652(17)	–0.15900(14)	0.52917(14)	0.2500	0.9278(2)
C6	0.53517(18)	0.59693(18)	–0.12595(16)	0.47223(14)	0.2500	1.0267(2)
C7	0.3949(2)	0.5534(3)	–0.1836(2)	0.49283(16)	0.2500	1.1608(3)
H7A	0.3718	0.5025	–0.1357	0.4987	0.3684	1.1891
H7B	0.3852	0.5032	–0.2453	0.5386	0.1877	1.1718
H7C	0.3374	0.6264	–0.2069	0.4545	0.1939	1.2083
C8	0.97867(18)	0.66997(17)	–0.05916(15)	0.51661(13)	0.2500	0.5886(2)
C9	1.1057(2)	0.6609(2)	–0.06907(18)	0.56367(17)	0.2500	0.4740(3)
H9A	1.1107	0.7285	–0.1146	0.5743	0.1316	0.4501
H9B	1.1105	0.5799	–0.1003	0.6093	0.3105	0.4906
H9C	1.1782	0.6682	0.0012	0.5377	0.3079	0.4077
C10	0.5196(3)	0.7919(3)	0.0747(2)	0.27934(14)	0.2500	1.0366(3)
H10A	0.5890	0.7503	0.1348	0.2455	0.2689	1.1044
H10B	0.4467	0.8102	0.0925	0.2688	0.1393	0.9982
H10C	0.5527	0.8701	0.0589	0.2737	0.3418	0.9763
C11	1.0446(2)	0.9154(2)	0.12911(18)	0.33816(17)	0.2500	0.4653(3)
H11A	0.9638	0.9601	0.0867	0.3202	0.3631	0.4898
H11B	1.1172	0.9749	0.1554	0.3200	0.1631	0.5222
H11C	1.0371	0.8747	0.1892	0.3210	0.2238	0.3826

[i] *x*, –*y*+1/2, *z*.

seems only a little better than B3LYP for the bond angles, the RMSE difference between these two methods being ca. 0.02°. The same trend was not observed for compound **2**. This time, both bond lengths and bond angles obtained by the HF method show the strongest correlation with the experimental values.

When the X-ray structures of the compounds are compared with its optimized counterparts (Figs. 3 and 4), slight conformational discrepancies are observed between them. In the solid state
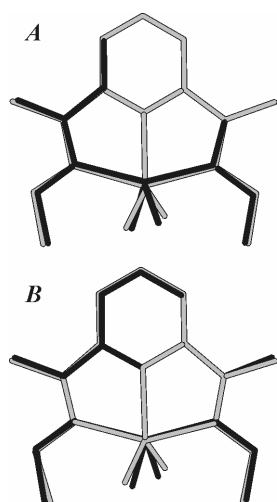
Fig. 3. Atom-by-atom superimposition of the calculated structures (red) [A = HF/LANL2DZ, B = = B3LYP/LANL2DZ] over the X-ray structure (black) for compound **1**. Hydrogen atoms omitted for clarity
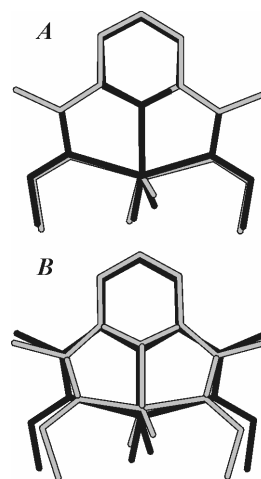

Fig. 4. Atom-by-atom superimposition of the calculated structures (red) [A = HF/LANL2DZ, B = = B3LYP/LANL2DZ] over the X-ray structure (black) for compound **2**. Hydrogen atoms omitted for clarity

structure of compound **1,** the dihedral angle between the five-membered chelate rings formed by Cu1/N1/C1/C8/N3 atoms and Cu1/N1/C5/C6/N2 atoms is 2.37(10)°, which has been calculated at 0.001° and 0.006° for HF and B3LYP respectively. This dihedral angle is 0° for the solid state structure of compound **2**, since the molecule lies with all non-H atoms, except the Cl1 atom, on a crystallographic mirror plane so that the complex is strictly planar. However, the angle is computed as 0.316° and 0.007° for HF and B3LYP respectively.
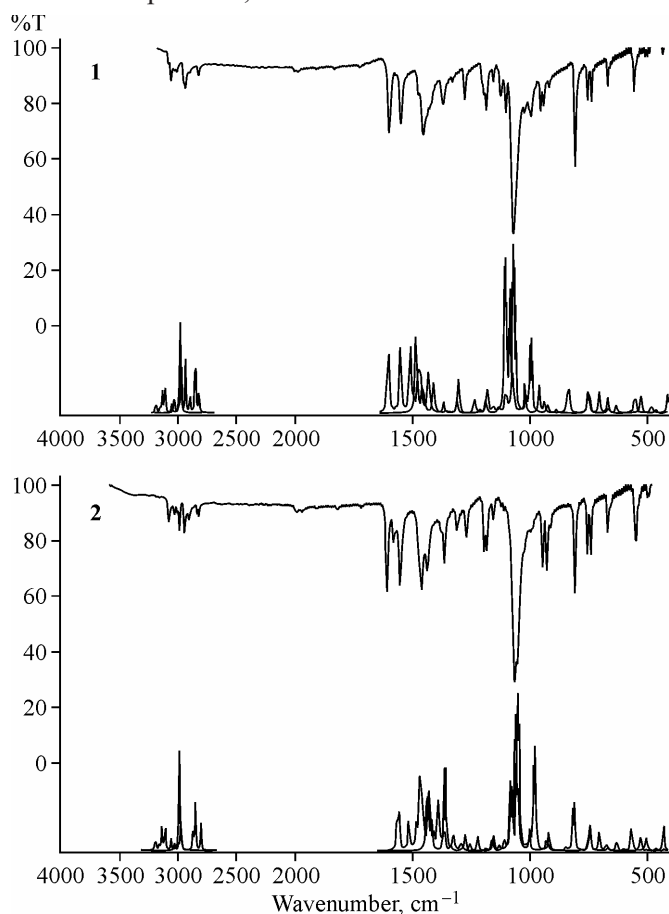
Five-coordinate complexes have geometries ranging from trigonal-bipyramidal to square-pyramidal. The information can be obtained by determining the structural index τ, which represents the relative amount of trigonality [for an ideal square pyramid $\tau = 0$ and for an ideal trigonal bipyramid $\tau = 1$; $\tau = (\beta-\alpha)/60°$, α and β being the two largest angles around the central atom] [26]. The values of τ for compounds **1** and **2** are 0.53 and 0.46 respectively, whereas it is found to be 0.28 and 0.33 for HF and B3LYP respectively in the case of compound **1**, and 0.26 and 0.44 for HF and B3LYP respectively in the case of compound **2**.

A logical method to globally compare the structures obtained by the theoretical

Fig. 5. Experimental and theoretical FT—IR spectra of compounds **1** and **2** (black = experimental, red = HF and blue = DFT/B3LYP)

T a b l e   2

Comparison of the Observed and Calculated
Vibrational Spectra of Compound **1**

Assignments	Experimental IR with KBr (cm^{-1})	Calculated (cm^{-1}) (LANL2DZ)	
		HF	B3LYP
ν_s C—H	3066	3038	3176
ν_{as} C—H	3035	3034	3169
ν_{as} C—H	3016	3000	3141
ν_{as} C—H$_3$	2943	2948	3123
ν_s C—H$_3$	2828	2847	2985
ν C=N	1603	—	1593
ν C=C	1552	1470	1585
α C—H$_3$	1457	1466	1455
α C—H$_3$	1440	1443	1440
α C—H$_3$	1372	1392	1416
ν C—CH$_3$ + γ C—H	1280	1289	1296
ω C—H$_3$	1188	1169	1176
γ C—H	1159	1145	1166
δ C—H$_3$	1125	1124	1134
γ C—H	1104	1105	1090
ν N—O	1071	1091	1056
ν O—CH$_3$	956	946	983

N o t e. Vibrational modes: ν, stretching; α, scissorring; γ, rocking; ω, wagging; δ, twisting.

A b b r e v i a t i o n s: s, symmetric; as, asymmetric.

T a b l e   3

Comparison of the Observed and Calculated
Vibrational Spectra of Compound **2**

Assignments	Experimental IR with KBr (cm^{-1})	Calculated (cm^{-1}) (LANL2DZ)	
		HF	B3LYP
ν_s C—H	3079	3031	3174
ν_{as} C—H	3030	3026	3142
ν_{as} C—H$_3$	2987	2983	3106
ν_{as} C—H$_3$	2947	2971	3097
ν_{as} C—H$_3$	2907	2890	3053
ν_s C—H$_3$	2837	2873	2991
ν_s C—H$_3$	2822	2829	2983
ν C=N	1610	—	1545
ν C=C	1582	—	1593
α C—H$_3$	1462	1466	1483
α C—H$_3$	1438	1443	1456
ν N—O	1065	1070	1060
γ C—H	991	1011	—
ν O—CH$_3$	947	940	989

N o t e. Vibrational modes: ν, stretching; α, scissoring; γ, rocking.

A b b r e v i a t i o n s: s, symmetric; as, asymmetric.

calculations is to superimpose the molecular skeleton onto that obtained from X-ray diffraction, giving an RMSE of 0.141 Å for HF and 0.147 Å for B3LYP calculations (Fig. 3) in the case of compound **1**, and 0.137 Å for HF and 0.334 Å for B3LYP calculations (Fig. 4) in the case of compound **2**. According to these results, it is seen that the results of the HF method have shown better fit to experimental ones than B3LYP in evaluating the geometrical parameters.

IR spectroscopy. The IR spectra of the title compounds were recorded in the range of 4000—400 cm^{-1} with a Bruker Vertex 80v FT—IR spectrometer using KBr pellets and are given in Fig. 5. We have calculated the theoretical vibrational spectra of the title compounds using both HF and B3LYP methods with the LANL2DZ basis set and compared with the experimental results. Theoretical and experimental results of the title compound are shown in Tables 2 and 3. The vibrational band assignments have been made using the GaussView molecular visualization program [22].

In the IR spectra of compound **1**, the asymmetric and symmetric aliphatic ν C—H stretching vibrations of the C—H$_3$ groups are observed at 2943 cm^{-1} and 2828 cm^{-1} respectively. These bands have been calculated at 2948 cm^{-1} and 2847 cm^{-1} for HF and at 3123 cm^{-1} and 2985 cm^{-1} for B3LYP. The band observed at 1586 cm^{-1} is assigned to the ν (C=N) stretching mode of the azomethine groups of the ligand. This band is shifted towards higher frequencies (1603 cm^{-1}) in the complex spectra, suggesting that the azomethine nitrogen atom is involved in the coordination process, and it has appeared at 1593 cm^{-1} for only B3LYP in the theoretical spectra of the complex. The experimental C=C stretching vibration is observed at 1552 cm^{-1}, which has been calculated at 1470 cm^{-1} for HF and 1585 cm^{-1} for B3LYP. Finally, the experimental N—O and O—CH$_3$ stretching modes belonging to the methyloxime groups, appeared at 1071 cm^{-1} and 956 cm^{-1} respectively, have been calculated at 1091 cm^{-1} and 946 cm^{-1} for HF and at 1056 cm^{-1} and 983 cm^{-1} B3LYP respectively.

In the IR spectra of compound **2**, the asymmetric and symmetric aliphatic v C—H stretching vibrations of the C—H_3 groups are observed in the range 2987—2822 cm^{-1}. However, these vibrations have been calculated theoretically in the 2983—2829 cm^{-1} range for HF and in the 3106—2983 cm^{-1} range for B3LYP. The v (C=N) stretching mode of the azomethine groups of the ligand shifted towards higher frequencies (1610 cm^{-1}) in the complex spectra, indicating that the azomethine nitrogen atom is involved in the coordination process, and it has appeared at 1545 cm^{-1} only for B3LYP in the theoretical spectra of the complex. The experimental C=C stretching vibration is observed at 1582 cm^{-1}, which has been calculated at 1593 cm^{-1} for B3LYP. Finally, the experimental N—O and O—CH_3 stretching modes belonging to the methyloxime groups, appeared at 1065 cm^{-1} and 947 cm^{-1} respectively, have been calculated at 1070 cm^{-1} and 940 cm^{-1} for HF and at 1060 cm^{-1} and 989 cm^{-1} B3LYP respectively.

To make a comparison with the experimental observations, we studied the correlation between the calculated and experimental data and obtained a correlation coefficient of 0.99907 for HF/LANL2DZ and 0.99926 for B3LYP/LANL2DZ in the case of compound **1**, and 0.99934 for HF/LANL2DZ and 0.99898 for B3LYP/LANL2DZ in the case of compound **2**. According to these results, it is seen that the results of the B3LYP method for compound **1** and the results of the HF method for compound **2** have shown better fit to the experimental ones compared with the other methods in the evaluation of vibrational frequencies.

Total energies and dipole moments. To investigate the behaviors of the total energy and dipole moment of the title compounds in solvent media, we have carried out the optimization calculations in three solvents (chloroform, methanol, water) at the B3LYP/LANL2DZ level using Onsager and PCM methods; the results are given in Table 4.

As can be seen from Table 4, the total energies of the title compounds obtained by Onsager and PCM models decrease with increasing polarity of the solvent so that the stability of the title compounds increases. The energy difference between the gas phase and the solvent media was found to be significant for both methods. The PCM method supplied more a stable structure than Onsager′s method with increasing polarity of the solvent. The trend in the total energies is also observed in the dipole moments. The dipole moments calculated by the PCM method are larger than those of the Onsager method in different solvents, and the dipole moments obtained for two solvation methods increase with the increase in the solvent polarity.

Molecular electrostatic potential. The molecular electrostatic potential, $V(\mathbf{r})$, at a given point $r(x, y, z)$ in the vicinity of a molecule, is defined in terms of the interaction energy between the electrical charge generated from the molecule electrons and nuclei and a positive test charge (a proton) located at $\mathbf{r}$. For the system studied the $V(\mathbf{r})$ values were calculated, as described previously, using the equation [27]

T a b l e 4

Total Energies and Dipole Moments of the Title Compounds in Different Solvents

Method	ε	Energy (a.u.)	ΔE (kcal/mol)	μ (Debye)	ε	Energy (a.u.)	ΔE (kcal/mol)	μ (Debye)
		Compound **1**				Compound **2**		
B3LYP	1	−968.85101297		8.7583	1	−917.81614015		7.3846
Onsager	4.90	−968.85827037	−4.554	13.1016	4.90	−917.81975114	−2.266	9.6130
	32.63	−968.86231069	−7.089	15.2972	32.63	−917.82143239	−3.321	10.6712
	78.39	−968.86285270	−7.430	15.5832	78.39	−917.82164588	−3.455	10.8064
PCM	4.90	−968.87714850	−16.400	13.6136	4.90	−917.83974270	−14.811	10.7858
	32.63	−968.88906532	−23.878	15.5325	32.63	−917.85061529	−21.633	12.3333
	78.39	−968.89089040	−25.023	15.8467	78.39	−917.85254796	−22.846	12.6531

N o t e. $\Delta E = E_{Solvation} - E_{Gas}$; ε = dielectric constant.

Fig. 6. Molecular electrostatic potential maps plotted on the surfaces of the title compounds with an isodensity value of 0.0004 a.u. calculated at the B3LYP/LANL2DZ level

1

−0.060   0   0.050 a.u.

$$V(\mathbf{r}) = \sum_{A} \frac{\mathbf{Z}_A}{|\mathbf{R}_A - \mathbf{r}|} - \int \frac{\rho(\mathbf{r}')}{|\mathbf{r}' - \mathbf{r}|} d\mathbf{r}'$$

where $\mathbf{Z}_A$ is the charge of the nucleus A located at $\mathbf{R}_A$, $\rho(\mathbf{r}')$ is the electron density function of the molecule, and $\mathbf{r}'$ is the dummy integration variable.

The molecular electrostatic potential (MEP) is related to the electron density and is a very useful descriptor to understand the sites for electrophilic attack and nucleophilic reactions as well as hydrogen bonding interactions [28]. The electrostatic potential is not always reliable for electrophilic and nucleophilic attack, but is more reliable for approach and thus noncovalent interactions [29].

2

−0.060   0   0.051 a.u.

To predict the reactive sites for electrophilic and nucleophilic attack for the title molecules, MEP was calculated at the B3LYP/LANL2DZ optimized geometry. The negative (red color) regions of MEP were related to electrophilic reactivity and the positive (blue color) ones to nucleophilic reactivity shown in Fig. 6. As can be seen in Fig. 6, the negative regions are localized on the chlorine atoms with a maximum value of –0.060 a.u. for both compounds. However, maximum positive regions are associated with the pyridine and methyl H atoms indicating possible sites for nucleophilic attack with a maximum value of 0.050 a.u. for compound **1** and 0.051 a.u. for compound **2**. These results supply information about the region from where the compounds can have intermolecular interaction and metallic bonding. Since the title compounds were stabilized by intra- and intermolecular C—H···Cl hydrogen bonds [11, 12], Fig. 6 supports the existence of these interactions observed in the solid state.

Frontier molecular orbitals analysis. The frontier molecular orbitals play an important role in the electric and optical properties, as well as in UV—Vis spectra and chemical reactions [30]. Figs. 7 and 8 show the distributions and energy levels of the α (spin-up) and β (spin-down) HOMO-LUMO orbitals computed at the B3LYP/LANL2DZ level for the title compounds.

As can be seen from Fig. 7, both of HOMOs consist of *M*—Cl antibonding orbitals of the π type. However, LUMOs are partially localized on the different parts of compound **1**. The LUMO α orbital is almost delocalized among the all atoms and mostly the π-antibonding type orbitals with some contributions from *M*—Cl σ-bonding orbitals, while the LUMO β orbital consists of *M*—Cl and *M*—N bonding orbitals of the σ type. For compound **2** (Fig. 8), the HOMO α orbital consists of *M*—Cl π-antibonding and *M*—N$_{pyridine}$ σ-bonding type orbitals, while the HOMO β orbital mainly consists of *M*—Cl and *M*—N$_{pyridine}$ π-antibonding type orbitals. However, both of the LUMOs are almost spread over all atoms and mostly the π-antibonding type orbitals with some contributions from *M*—Cl σ-bonding orbitals. The value of the energy separation between the HOMO and LUMO is 3.240 eV for α orbitals and 2.647 eV for β orbitals in the case of compound **1**, and 3.140 eV for α orbitals and 3.021 eV for β orbitals in the case of compound **2**. These energy gaps are in agreement with the value of 2—3 eV often encountered for stable transition metal complexes [31].

CONCLUSIONS

In this study, the structural parameters and IR wavenumbers of two 2,6-diacetylpyridine bis(*O*-methyloxime) complexes were calculated using the HF and DFT(B3LYP) methods with the LANL2DZ basis set, and compared with the experimental data. For the geometrical parameters, the results of the HF method have shown a better fit to experimental ones than those of the B3LYP
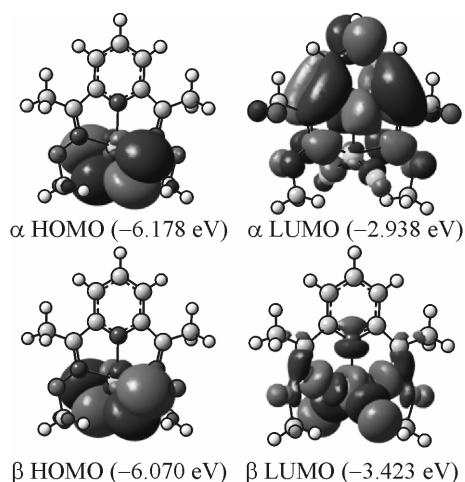
α HOMO (−6.178 eV)   α LUMO (−2.938 eV)

β HOMO (−6.070 eV)   β LUMO (−3.423 eV)
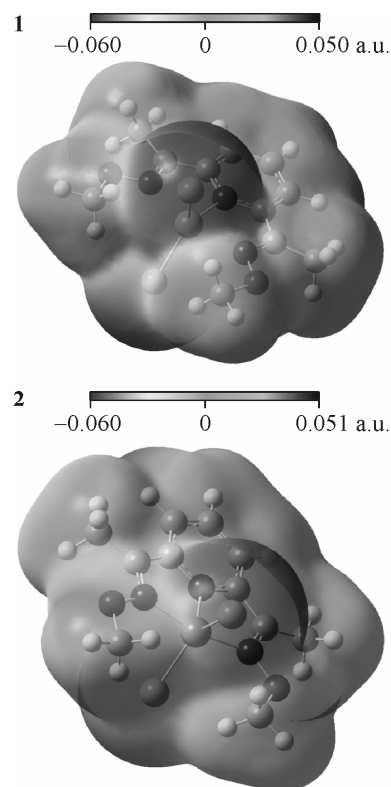
Fig. 7. Molecular orbital surfaces and energy levels given in parentheses for the α (spin-up) and β (spin-down) HOMO-LUMO of compound **1** computed at the B3LYP/LANL2DZ level. The positive phase is red, and the negative phase is green
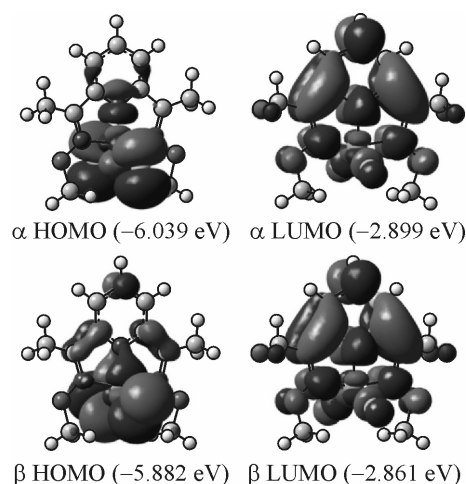

α HOMO (−6.039 eV)   α LUMO (−2.899 eV)

β HOMO (−5.882 eV)   β LUMO (−2.861 eV)

Fig. 8. Molecular orbital surfaces and energy levels given in parentheses for the α (spin-up) and β (spin-down) HOMO-LUMO of compound **2** computed at the B3LYP/LANL2DZ level. The positive phase is red, and the negative phase is green

method. It was noted here that the experimental results belong to the solid phase and theoretical calculations belong to the gaseous phase. In the solid state, the existence of the crystal field along with the intermolecular interactions have connected the molecules together, which resulted in the differences between the calculated and experimental bond parameters. It is seen from the theoretical results that the B3LYP method for compound **1** and the HF method for compound **2** seem to be more appropriate than the other methods for the calculation of vibrational frequencies. The MEP maps agree well with the solid-state interactions. The total energies of the title compounds decrease with increasing polarity of the solvent and the stability of the title compound increases in going from the gas phase to the solution phase.

REFERENCES

1. *Small B.L., Brookhart M.* // J. Amer. Chem. Soc. – 1998. – **120**. – P. 7143 – 7144.
2. *Small B.L., Brookhart M.* // Macromolecules. – 1999. – **32**. – P. 2110 – 2119.
3. *Britovsek G.J.P., Gibson V.C., Kimberley B.S.* // J. Amer. Chem. Soc. – 1999. – **121**. – P. 8728 – 8740.
4. *Tellmann K.P., Gibson V.C., White A.J.P., Williams D.J.* // Organometallics. – 2005. – **24**. – P. 280 – 286.
5. *Griffiths E.A.H., Britovsek G.J.P., Gibson V.C., Gould I.R.* // Chem. Commun. – 1999. – **14**. – P. 1333 – 1334.
6. *Dias E.L., Brookhart M., White P.S.* // J. Chem. Soc. Chem. Commun. – 2001. – **5**. – P. 423 – 424.
7. *Çetinkaya B., Çetinkaya E., Brookhart M., White P.S.* // J. Mol. Catal. A. – 1999. – **142**. – P. 101 – 112.
8. *Gibson V.C., Spitzmesser S.K.* // Chem. Rev. – 2003. – **103**. – P. 283 – 316.
9. *Gibson V., Wass D.* // Chem. Br. – 1999. – **7**. – P. 20 – 23.
10. *Bennett A.M.A.* // Chemtech. – 1999. – **29**. – P. 24 – 28.
11. *Özdemir N., Dinçer M., Dayan O., Çetinkaya B.* // Acta Crystallogr. – 2006. – **C62**. – P. m315 – m318.
12. *Özdemir N., Dinçer M., Dayan O., Çetinkaya B.* // Acta Crystallogr. – 2006. – **C62**. – P. m398 – m400.
13. *Scott A.P., Radom L.* // J. Phys. Chem. – 1996. – **100**. – P. 16502 – 16513.
14. *Ricca A., Bauschlicher C.W. Jr.* // J. Phys. Chem. – 1995. – **99**. – P. 9003 – 9007.
15. *Wadt W.R., Hay P.J.* // J. Chem. Phys. – 1985. – **82**. – P. 284 – 298.
16. *Hay P.J., Wadt W.R.* // J. Chem. Phys. – 1985. – **82**. – P. 299 – 310.
17. *Lee C., Yang W., Parr R.G.* // Phys. Rev. B. – 1988. – **37**. – P. 785 – 789.
18. *Becke A.D.* // J. Chem. Phys. – 1993. – **98**. – P. 5648 – 5652.
19. *Hay P.J., Wadt W.R.* // J. Chem. Phys. – 1985. – **82**. – P. 270 – 283.

20. *Dhumal N.R., Gejji S.P.* // J. Mol. Struct. (Theochem.). – 2008. – **859**. – P. 86 – 92.

21. *O'Boyle N.M., Albrecht T., Murgida D.H. et al.* // Inorg. Chem. – 2007. – **46**. – P. 117 – 124.

22. *Dennington R. II, Keith T., Millam J.* GaussView version 4.1.2, Semichem, Inc., Shawnee Mission KS, 2007.

23. *Frisch M.J., Trucks G.W., Schlegel H.B., Scuseria G.E., Robb M.A., Cheeseman J.R., Montgomery J.A. Jr., Vreven T., Kudin K.N., Burant J.C., Millam J.M., Iyengar S.S., Tomasi J., Barone V., Mennucci B., Cossi M., Scalmani G., Rega N., Petersson G.A., Nakatsuji H., Hada M., Ehara M., Toyota K., Fukuda R., Hasegawa J., Ishida M., Nakajima T., Honda Y., Kitao O., Nakai H., Klene M., Li X., Knox J.E., Hratchian H.P., Cross J.B., Bakken V., Adamo C., Jaramillo J., Gomperts R., Stratmann R.E., Yazyev O., Austin A.J., Cammi R., Pomelli C., Ochterski J.W., Ayala P.Y., Morokuma K., Voth G.A., Salvador P., Dannenberg J.J., Zakrzewski V.G., Dapprich S., Daniels A.D., Strain M.C., Farkas O., Malick D.K., Rabuck A.D., Raghavachari K., Foresman J.B., Ortiz J.V., Cui Q., Baboul A.G., Clifford S., Cioslowski J., Stefanov B.B., Liu G., Liashenko A., Piskorz P., Komaromi I., Martin R.L., Fox D.J., Keith T., Al-Laham M.A., Peng C.Y., Nanayakkara A., Challacombe M., Gill P.M.W., Johnson B., Chen W., Wong M.W., Gonzalez C., Pople J.A.* Gaussian 03 revision E.01, Gaussian, Inc., Wallingford CT, 2004.

24. *Onsager L.* // J. Amer. Chem. Soc. – 1936. – **58**. – P. 1486 – 1493.

25. *Tomasi J., Mennucci B., Cammi R.* // Chem. Rev. – 2005. – **105**. – P. 2999 – 3094.

26. *Addison A.W., Rao T.N., Reedijk J. et al.* // J. Chem. Soc. Dalton Trans. – 1984. – **7**. – P. 1349 – 1356.

27. *Politzer P., Murray J.S.* // Theor. Chem. Acc. – 2002. – **108**. – P. 134 – 142.

28. *Okulik N., Jubert A.H.* // Internet Electron. J. Mol. Des. – 2005. – **4**. – P. 17 – 30.

29. *Politzer P., Murray J.S., Concha M.C.* // Int. J. Quantum. Chem. – 2002. – **88**. – P. 19 – 27.

30. *Fleming I.* Frontier Orbitals, Organic Chemical Reactions, Wiley, London, 1976.

31. *Blower P.J., Dilworth J.R., Maurer R.I. et al.* // J. Inorg. Biochem. – 2001. – **85**. – P. 15 – 22.